Nonstretch NMO

Hervé Perroud (IGP, University of Pau, Av. de l'Université, 64013 Pau Cedex, France) and
Martin Tygel (LGC, State University of Campinas, CP 6065, CEP 13081-970, Campinas, Brazil)

Copyright 2003, SBGf - Sociedade Brasileira de Geofísica

This paper was prepared for presentation at the 8th International Congress of The Brazilian Geophysical Society held in Rio de Janeiro, Brazil, 14-18 September 2003.

Contents of this paper was reviewed by The Technical Committee of The 8th International Congress of The Brazilian Geophysical Society and does not necessarily represents any position of the SBGf, its officers or members. Electronic reproduction, or storage of any part of this paper for commercial purposes without the written consent of The Brazilian Geophysical Society is prohibited.

Abstract

We describe a new implementation of the normal-moveout (NMO) correction, that is routinely applied to common-midpoint (CMP) reflections prior stacking. The procedure, called nonstretch NMO, automatically avoids the undesirable stretch effects that are present in conventional NMO. Under nonstretch NMO, a significant range of large offsets, that would normally be muted in the case of conventional NMO, can be kept and used, leading to better stack and velocity determinations. We illustrate the use of nonstretch NMO by its application to a real ground-penetrating radar (GPR) dataset.

INTRODUCTION

As shown firstly by Buchholtz (1972), conventional application of NMO correction to a CMP reflection generates a stretch which increases with offset and decreases with zero-offset time. The discussion on the effect of NMO correction on reflection data has always been a topic of interest. For our needs, we cite one of the earliest references (Dunkin and Levin, 1973). Due to stretch, a number of NMO-corrected traces needs to be muted after a given offset. For this purpose, an acceptable stretch limit has to be fixed by the user, and the choice of this limit could have a great impact on the frequency content of the stack images (Miller, 1992). As a consequence, the large-aperture traces cannot be used in velocity analysis and stacking processes. This is particularly harmful for shallow reflectors, which present relatively large offsets with respect to depth (or traveltime). It can also be a significant handicap for the search of subtle traps (Noah, 1996).

The origin of the NMO stretch lies in the form of the hyperbolic equation

$$t^2(h) = t_0^2 + 4h^2/v_{nmo}^2, \qquad (1)$$

that is used to describe the reflection time t as a function of half-offset, h. Here, t_0 stands for the zero-offset (ZO) traveltime and v_{nmo} represents the NMO velocity, which is an estimation of the root-mean-square (RMS) velocity in the case of flat-layered media. From simple geometrical considerations, it can be verified that equation (1) represents a hyperbola whose asymptote passes through the origin and has slope equal to $2v_{nmo}^{-1}$. For a band-limited source pulse, the reflection event of traveltime (1) is generally observed as a strip of constant width (the pulse width) around that curve. The ideal NMO correction should be the one that would simply move the whole strip around the traveltime curve (1) onto a corresponding strip (of the same width) around the horizontal line $t = t_0$.

For a user-selected value of t_0, an estimation of v_{nmo} is conducted as a one-parameter search that maximizes the coherency (semblance) of the data within the CMP gather. The procedure is usually called NMO velocity analysis, or velocity scan. After an acceptable estimate of v_{nmo} is obtained, conventional NMO correction transforms samples $t(h) + \tau$ in the vicinity of the traveltime curve (1) onto their corresponding values $t_0 + \tau'$ according to the equation

$$(t_0 + \tau')^2 = (t(h) + \tau)^2 - 4h^2/v_{nmo}^2. \qquad (2)$$

Comparison of equations (1) and (2) yields the well-known first-order relationship $\tau'/\tau = t(h)/t_0$ (Dunkin and Levin, 1973), which defines the stretch ratio. To understand why the conventional NMO correction, as provided by equation (2), introduces a stretch in the output signal, we refer to Fig. 1, (left). There we see that, for fixed v_{nmo}, the NMO traveltime curves for zero-offset times t_0 and $t_0 + \tau$ are both converging, for large offsets, towards their common asymptote $t = 2h.v_{nmo}^{-1}$. This means that these hyperbolae are not parallel to each other: after moveout, the shape of the reflection pulse will therefore be stretched since, within the same trace, smaller time samples will experience a larger moveout than larger time samples. As seen from the above analysis, one approach to avoid the NMO stretch, is to introduce a different traveltime moveout expression that keeps as much as possible the parallelism between the hyperbolae when changing zero-offset time. This idea was proposed by de Bazelaire (1988) with the so-called method of shifted hyperbolae. In this formulation, the scanned parameter is the focussing time of the hyperbola, t_p, instead of the velocity v_{nmo}. Another approach was introduced as the block-move-sum (BMS) concept (Rupert and Chun, 1975), which applies a series of static shifts to blocks of data, followed by a summation. BMS has been the subject of further developments, as recently illustrated by Brouwer (2002), where an up-to-date references list can be found.

In the present paper, however, we want to stay as close as possible to the widely used NMO method and traveltime equation (1), so that our new approach can be adopted by the users of the traditional NMO without a severe change of processing tools and habits.

NONSTRETCH NMO

As stated above, to avoid stretch, one has to keep parallelism of NMO traveltimes as much as possible. However, strict (global) parallelism is not achievable using the classical NMO equation (1), since their asymptotes intersect at the origin. So the problem can be formulated in the following manner: what condition should we impose such that the NMO for a single trace can be performed without stretch? The only parameter that has some degree of freedom is the v_{nmo}, which is also related to the slope of the asymptote. Nonstretch NMO, therefore, proposes to adjust it so that local parallelism can be obtained. To explain how this can be done, we refer to Fig. 1, (right), and consider the equation

$$(t(h)+\tau)^2 = (t_0+\tau)^2 + 4h^2/v^2(\tau). \qquad (3)$$

Here, τ is a time shift and $v(\tau)$ is the adjusted velocity that eliminates the stretch for that half-offset h. Note that equation (3) is the same as equation (2), with the exception that the adjusted velocity, $v(\tau)$, replaces the fixed NMO-velocity, v_{nmo}, and the non-stretch condition, $\tau' = \tau$, has been imposed. After simple manipulations combining equations (1) and (3), we obtain the important expression

$$v(\tau) = v_{nmo}\left(1+\frac{2\tau}{t(h)+t_0}\right)^{-1/2} \qquad (4)$$

that determines the adjusted velocity $v(\tau)$ for a reflection event, characterized by t_0 and v_{nmo}, at offset h and time shift τ. To better reveal the physical meaning of equation (4), it is useful to recast it in the form

$$v(\tau) = v_{nmo}\left(1+\frac{2}{1+\sqrt{1+a^2}}\frac{\tau}{t_0}\right)^{-1/2}, \qquad (5)$$

where

$$a = \frac{2h}{t_0.v_{nmo}} \qquad (6)$$

is the geometrical aperture in an effective medium defined by t_0 and v_{nmo}. Under the usual assumption of a constant-velocity flat-layered model, the geometrical aperture a is simply the tangent of the incidence angle onto an effective reflector at depth $v_{nmo}t_0/2$ for a source-receiver pair with half-offset h. In such a media, the NMO stretch factor is linked to the aperture a by the formula $\tau'/\tau = t(h)/t_0 = \sqrt{1+a^2}$. This makes explicit the relationship between the NMO stretch and the nonstretch NMO adjusted velocity.

Equation (5) better displays the main factors that influence the determination of $v(\tau)$, namely the zero-offset time of the event t_0 and the geometrical aperture a. For a given event, the strongest effect onto the stacking velocity corresponds to null aperture ($a = 0$), where equation (5) reduces to

$$v(\tau) = v_{nmo}\left(1+\frac{\tau}{t_0}\right)^{-1/2} \qquad (7)$$

It corresponds to maintain constant the product $(t_0+\tau)v(\tau)^2$, and thus the curvature of the hyperbolic traveltime curves at null offset. On the other hand, if the aperture a gets very large, equation (5) tends to its limiting value $v(\tau) = v_{nmo}$, which means that v_{nmo} has to be kept constant over the whole pulse length. For the intermediate, more usual, apertures, the adjusted velocity lies between these two extreme cases. Moreover, it can be seen from equation (4) that, for the set of events recorded on a given trace, stronger effects onto the stacking velocity are observed at shorter zero-offset times.

From equation (4), as $t(h)$ and t_0 are strictly positive, we see that $v(\tau)$ always decreases when the time shift τ increases. Therefore, even setting NMO velocity constant is not sufficient to avoid stretch, as done in the constant-velocity-stack (CVS) approach. In addition, the classical increase of NMO velocity with time that results from interpolating the time-velocity distribution is going the wrong way and further increases the stretch effect of the NMO.

Based on the above considerations, we propose the following scheme to implement the nonstretch NMO. After performing the usual NMO velocity analysis, which estimates t_0 and v_{nmo} for each reflection event, a specific velocity distribution is constructed for each trace in the following manner: for each event, the originally picked time-velocity point is replaced by a curve segment which follows equation (4) (see Fig. 2, left). Note that the only quantity that is additionally needed is the range for argument τ. A good estimation of this range can be obtained as the inverse of the bandwidth of the propagating signal. In this way, the whole procedure can be made automatically. Obviously, the trace-dependent, time-velocity distribution obtained here is solely used for applying the nonstretch NMO correction and should be discarded after this purpose. As the non-stretch condition implies that the velocity decreases with time in the τ-range, it means that the interpolated NMO velocity between events will grow more rapidly, and thus the NMO stretch effect will be increased between events. It is therefore necessary not to forget any reflection event in the velocity picking, so that the increased stretch will concern only the noise between events.

The classical NMO processing tools usually provide an upper limit to acceptable stretch, the stretch-mute ratio, all samples with a NMO stretch exceeding this ratio being simply muted. This mute renders impossible an exact inverse NMO process, opposite to the case of nonstretch NMO. This new process can therefore be quite helpful for any processing chain in which NMO can be temporarily applied,

and later removed.

However, for the large apertures encountered in near surface seismics or GPR studies, NMO stretch leads to a very severe mute of superficial events. This results on a blind zone at the top of the sections. On the other hand, the stretch-mute ratio provides a way to limit the offset used in the CMP gather analysis and stack, and therefore acts as an implicit trace filter. When applying the proposed nonstretch NMO, new problems are bound to arise with long offsets, as for example interferences between crossing events. As shown in the example below, a way to circomvent these situations is to process the reflection events one at a time. To do so, we construct the hyperbolae corresponding to the onset of each event from the time-velocity distribution obtained by the NMO velocity scan. Then, for each event, we mute all samples above the corresponding hyperbola and below those for the next events and apply the nonstretch NMO. As each event is processed individually, the modified velocity distribution needs not to be interpolated between events. It is simply extrapolated to the full time range (see Fig. 2, right). As a consequence, this limits the stretch induced by NMO *between* events. Furthermore, note that the NMO velocity above the event is the largest, and the one below the event is the smallest. As a consequence, there can be no fit between that event and the NMO stacking curves apart from those that refer to zero-offset traveltimes t_0 that belong to the very time range for that event. This approach is a natural solution to the crossing event problem (even if a part of the event is muted). A complete processed trace is later recovered by summing the contributions from all events. Note that since each event does not suffer from NMO stretch mute, inverse NMO should still be possible.

Application on a GPR real dataset

A test of this new approach for NMO was carried out on a real GPR multi-offset dataset, with offsets ranging from 0.6 m to 6 m, 28 fold, and penetration depth of about 5 m. The uppermost event corresponds to a maximum aperture of about 4, while it is less than 1 for the lowermost one. The results of both conventional (stretch-mute ratio 1.3) and nonstretch NMO on a single CMP gather are shown in Figure 3. Crossing events can be observed for large offsets. These were muted by conventional NMO, but correctly recovered by nonstretch NMO. It is to be noticed how different the stacked traces are in their uppermost part. This emphasizes the interest of this new process. In particular, one can observe that the event at time 0.05 ms has completely disappeared after conventional NMO, due to its phase shift with offset.

To check the potential of nonstretch NMO to improve the time images, it has been applied to all CMP gathers, spaced every 0.1 m along the 55 m of the GPR profile. Velocities were picked using a conventional semblance map, but were adjusted to best flatten the reflection events after nonstretch NMO, rather than conventional NMO. From these picked velocities, both conventional (stretch-mute ratio 1.5) and nonstretch NMO were applied. The resulting stack sections, after amplitude balancing, are displayed in Figure 4. Although the two sections bear strong resemblance, significant differences can still be observed. Firstly, the upper half of the stack section obtained with nonstretch NMO reveals, as expected, more focussed events, and a much clearer rendering of the channel filling in its right part. This is particularly significant since that part of the section has a lower signal-to-noise ratio, and therefore needs a larger number of traces to define a clear image. This is exactly what our new process provides. Second, all over the section, nonstretch NMO generates less smoothed images. As a matter of fact, conventional NMO section appears to be a smoothed version of its nonstretch NMO counterpart. It is interesting to note that the NMO stretch effect, which induces a dilution of the vertical resolution, also seems to generate a bit of horizontal smoothing.

To quantitatively evaluate the improvement on seismic resolution brougth by nonstretch NMO, we performed a spectral analysis of both stack sections. As the NMO stretch effect varies with time, the analysis was carried out on two time gates of equal duration, 0.06 microsecond, starting just below the top mute. The limit between these time-gates corresponds to a geometrical aperture around 1. Peak frequencies and frequency bandwidths estimated from these spectra, revealed that the greater change is obtained in the upper part of the sections. In that region, peak frequency increased from 102 Mhz to 119 Mhz, and bandwidth from 94 Mhz to 105 Mhz. In the lower part of the sections, no significant change can be noticed, apart from a slight increase (from 114 to 117 Mhz) of the peak frequency. As expected, nonstretch NMO appears to be most efficient when the seismic aperture is larger. In this way, it should be most helpful in near-surface geophysics, e.g. in seismics or GPR studies.

CONCLUSIONS

We presented a new method, called nonstretch NMO, that adapts the conventional NMO procedure with the aim of producing corrected traces with no stretch effects. In this way, the proposed method can be easily incorporated to the routine processing sequences, say in seismics or GPR investigations. To illustrate the method, we applied the procedure to a real (GPR) example. In that case study, the new method was able to significantly enlarge the offset range of the undistorted NMO corrected traces and thus improve the quality and resolution of the time images. It appears particularly useful when the geometrical aperture exceeds 1, e.g. when half-offset is larger than reflector depth. Also a number of remarks concerning the implementation have been made. This includes in particular the difficult case of crossing events.

ACKNOWLEDGEMENTS

We like to thank the Research Foundation of the State of São Paulo (FAPESP, Brazil), for financial support (Grant 01/01068-0) and the stay of H.P. at Unicamp, Campinas (Grant 02/06590-0). The idea to use the inverse of the signal bandwidth in the nonstretch NMO process was suggested by E. de Bazelaire. The GPR data were acquired and processed with the help of P. Senechal. All NMO and velocity scan procedures have been conducted with the Seismic Unix software, release 35.3, Center for Wave Phenomena, Colorado School of Mines. We finally thank C. Theodoro for useful discussions and J. Schmidt for encouragement and support.

References

Brouwer, J. H., 2002, Improved nmo correction with a specific application to shallow-seismic data: Geophys. Prosp., **50**, 225–237.

Buchholtz, H., 1972, A note on signal distortion due to dynamic (nmo) corrections: Geophys. Prosp., **20**, no. 02, 395–402.

de Bazelaire, E., 1988, Normal moveout revisited - Inhomogeneous media and curved interfaces: Geophysics, **53**, no. 02, 143–157.

Dunkin, J. W., and Levin, F. K., 1973, Effect of normal moveout on a seismic pulse: Geophysics, **38**, no. 04, 635–642.

Miller, R. D., 1992, Normal moveout stretch mute on shallow-reflection data: Geophysics, **57**, no. 11, 1502–1507.

Noah, J. T., 1996, Interpreter's corner - NMO stretch and subtle traps: The Leading Edge, **15**, no. 05, 345–347.

Rupert, G. B., and Chun, J. H., 1975, The block move sum normal moveout correction: Geophysics, **40**, no. 01, 17–24.

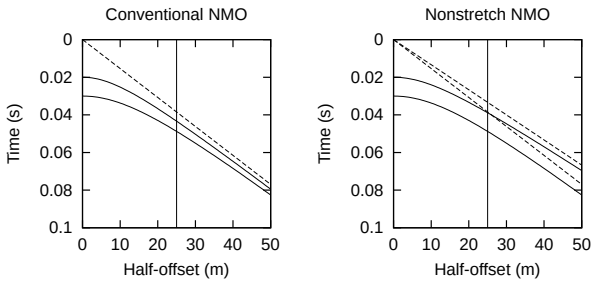

Figure 1: Comparison between conventional NMO (left) and nonstretch NMO (right). The hyperbolae corresponding to the onset and the end of a reflection event are shown (solid lines), together with their asymptotes (dashed lines). At half-offset h equal 25 m, the vertical line reveals the separation between the hyperbolae. For conventional NMO, the hyperbolae converge with h, while for nonstretch NMO, their distance is kept equal for the chosen h.

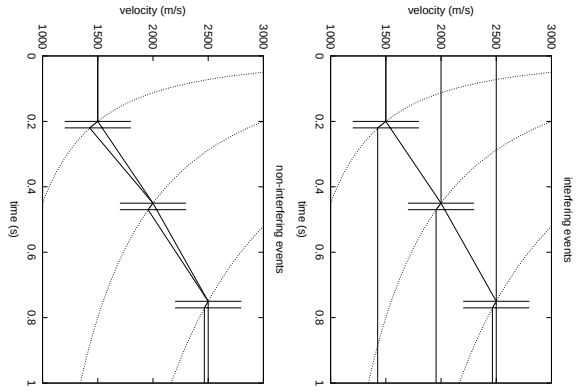

Figure 2: Construction of velocity distribution in the case of non-interfering (left) or interfering (right) events. Thick solid lines represent the modified velocity distributions that replace the corresponding conventional ones, shown as thin solid lines. Dotted lines represent the velocity functions derived from equation (4) for individually picked events, computed for half-offset h equal 200 m. They are used only in the time-range that refers to the pulse length between two horizontal bars.

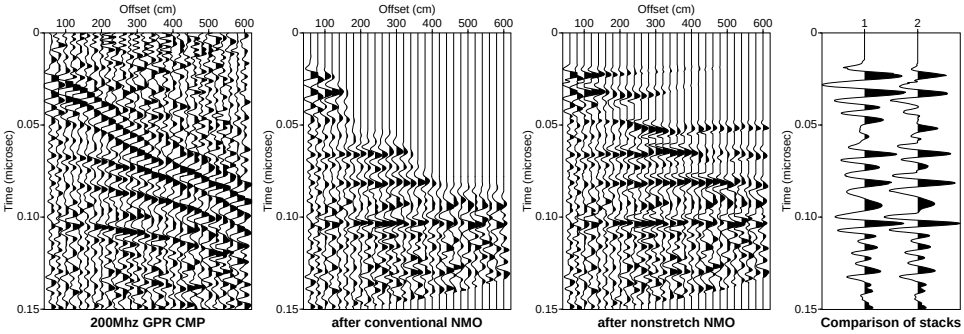

Figure 3: Comparison of conventional NMO and nonstretch NMO for a real GPR CMP gather. In the comparison of stacks, the left trace was obtained by conventional NMO, whereas the right one was obtained by nonstretch NMO.

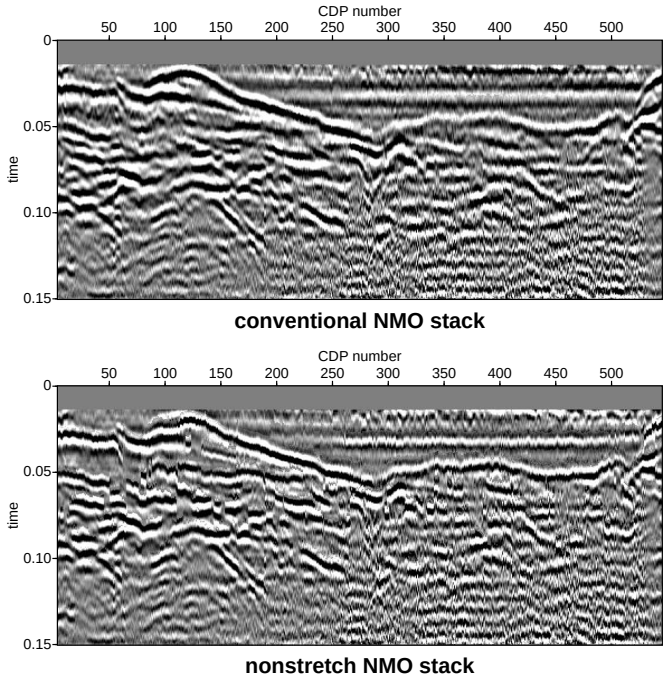

Figure 4: Comparison of conventional NMO and nonstretch NMO for a complete stack section. Trace amplitudes were balanced to better represent the kinematic aspects of the GPR images.